Materials Transactions, Vol. 42, No. 8 (2001) pp. 1535 to 1539
Special Issue on Nano-Metals I

Soft Magnetic Properties of Nanocrystalline Fe–Nb–B–P Alloys Produced in the Atmosphere by Melt-Spinning Method

Akinori Kojima[1], Satoru Ito[1], Akihiro Makino[2] and Akihisa Inoue[3]

[1]*Magnetic Application Dept. Alps Electric Co., Ltd., Nagaoka 940-8572, Japan*
[2]*Department of Machine Intelligence and System Engineering, Akita Prefectural University, Honjyo 015-0055, Japan*
[3]*Institute for Materials Research, Tohoku University, Sendai 980-8577, Japan*

The soft magnetic properties of nanocrystalline Fe–Nb–B and Fe–Nb–B–P alloys produced in the atmosphere by a melt-spinning method have been investigated. The nanocrystalline $Fe_{100-x-y}Nb_xB_y$ ternary alloys show good soft magnetic properties, relative permeability (μ') above 35000 at a frequency of 1 kHz and coercive force (H_c) below 5.0 Am^{-1}, as well as high saturation magnetic induction (B_s) above 1.55 T in the compositional range of $x = 6.5$–6.7 and $y = 9.3$–10.0 at%. The soft magnetic properties of the nanocrystalline Fe–Nb–B ternary alloys are improved by 0.5–1.5 at% substitution of P for B, without decreasing their B_s. The magnetostriction (λ_s) value increases and the mean grain size of bcc-Fe phase (D) decreases slightly by substitution of P for B. The nanocrystalline $Fe_{84}Nb_{6.5}B_9P_{0.5}$ and $Fe_{84}Nb_{6.5}B_{8.5}P_1$ alloys show good soft magnetic properties, μ' of 46000–47000 at a frequency of 1 kHz, H_c of 3.6–3.9 Am^{-1} and the core loss of the 0.09 Wkg^{-1} at maximum induction (B_m) of 1.33 T and a frequency of 50 Hz as well as high B_s of 1.60 T, suggesting that these nanocrystalline Fe–Nb–B–P alloys are suitable for a core materials for pole transformers.

(Received March 2, 2001; Accepted June 18, 2001)

Keywords: *high saturation magnetic induction, low core loss, nanocrystalline, crystallization, iron-niobium-boron-phosphorus alloy*

1. Introduction

In recent years, energy saving becomes a serious problem from the viewpoint of an environmental protection, so that core materials with low losses are demanded for pole transformers in order to reduce energy loss. Fe-based amorphous alloys are good candidates as a new core material for pole transformers because they show low core losses as well as a rather high magnetic induction (B_s). Thus, a conventional Fe–3.5%Si alloy now in use as a core material of the pole transformers, is replaced gradually by Fe-based amorphous alloys.

In the last decade, nanocrystalline melt-spun alloys produced by crystallization of an amorphous phase have been obtained and reported[1–3] to show excellent soft magnetic properties. In particular, the nanocrystalline Fe-rich Fe–M–B (M=Zr, Hf, Nb) ternary alloys,[2,3] which consist of bcc-Fe crystallites surrounded by a residual amorphous phase, show high relative permeability of 30000–50000 at 1 kHz and low coercive force of 4.8–5.3 Am^{-1} owing to magnetic coupling between crystalline grains through the ferromagnetic amorphous phase. Furthermore, these nanocrystalline Fe–M–B alloys show high B_s ranging from 1.5 to 1.7 T owing to the high Fe concentration. More recently, the nanocrystalline $Fe_{85.5}Zr_2Nb_4B_{8.5}$ quaternary alloy, which is synthesized by mixing the $Fe_{90}Zr_7B_3$ alloy with a slightly negative λ_s and the $Fe_{84}Nb_7B_9$ alloy with positive λ_s, has been reported[4,5] to show high permeability of 60000 at 1 kHz, high B_s of 1.64 T and zero magnetostriction. Therefore, the nanocrystalline Fe–M–B ternary and quaternary alloys attract a great interest as core materials for the pole transformers. These nanocrystalline Fe–M–B alloys are usually produced by melt-spinning in an Ar atmosphere and subsequent annealing. For practical use, such nanocrystalline alloys, showing good soft magnetic properties and high B_s simultaneously, are desired to be produced in the atmosphere by a melt-spinning method.

It has been already reported[6–9] that the addition of elements (*e.g.* Pd, Cu, Co, Ga, Ti, V, Cr and Mn) to the nanocrystalline Fe–M–B alloys improves their soft magnetic properties due to the decrease in the grain size of bcc-Fe phase or the magnetostriction. On the other hand, there are few reports about the effect of the addition of P to the nanocrystalline Fe–M–B alloys. In this paper, we present the magnetic properties of the nanocrystalline Fe–Nb–B and Fe–Nb–B–P alloys produced by melt-spinning in the atmosphere and subsequent annealing.

2. Experimental Procedure

Fe–Nb–B and Fe–Nb–B–P alloy ingots were prepared by induction melting in an Ar atmosphere. The rapidly solidified ribbons with 15 mm in width and 20–25 µm in thickness were produced in the atmosphere by a single-roller melt-spinning method. The as-quenched ribbons were mechanically punched to be used as samples. Annealing treatment was carried out by treating the samples for 300 s at temperatures (T_a) ranging from 820 to 970 K in a vacuum with a heating rate of 3 K/s.

The saturation magnetic induction (B_s) was measured under an applied field of 800 kAm^{-1} using a vibrating sample magnetometer (VSM). Density was measured by the Archimedian method. The permeability (μ') was measured at a frequency of 1 kHz under an applied field of 0.4 Am^{-1} with a vector impedance analyzer, and the coercive force (H_c) was measured under a maximum applied field of 800 Am^{-1} with a low frequency B-H loop tracer. The core loss (W) was measured at a frequency of 50 Hz with an AC B-H analyzer, and the saturation magnetostriction (λ_s) was measured under an applied field of 80 kAm^{-1} by a strain gage technique. These measurements were carried out at room temperature using disk-shaped samples with 6 mm in diameter for B_s and λ_s, and ring-shaped samples with a 6 mm inner diameter and a 10 mm outer diameter for μ', H_c and W. The crystallization temperature (T_x) of the amorphous alloys was determined by a differential thermal analyzer (DTA) at a heating rate of 0.17 Ks^{-1}. Microstructure was observed by a transmission electron microscope (TEM). The mean grain sizes of bcc-Fe phase are evaluated from the figure of X-ray diffraction (110) peak and the TEM images.

3. Results and Discussion

In general, the sheet alloys with more than 100 mm wide are necessary for producing the pole transformers, so it requires a large-scale melt-spinning apparatus. If the alloys are inactive in oxidation and can be produced in the atmosphere, we can make the melt-spinning apparatus simple because the evacuating system is unnecessary. Therefore, the soft magnetic ribbon alloys which can be made in the atmosphere by a melt-spinning method, are desirable for practical use. Nb element is relatively inactive in oxidation as compared with Zr and Hf, so that we chose the Fe–Nb–B system in Fe–M–B (M=Nb, Zr, Hf) in order to prepare the melt-spun samples in the atmosphere and investigate their magnetic properties and microstructure.

First, we have investigated the compositional dependence of the magnetic properties for the nanocrystalline $Fe_{100-x-y}Nb_xB_y$ (x = 5–7, and y = 9–11 at%) alloys. Figure 1(a) show the ternary diagram of permeability (μ') and saturation induction (B_s), and Fig. 1(b) shows that of coercive force (H_c) for the nanocrystalline Fe–Nb–B alloys produced by melt-spinning in the atmosphere and subsequent annealing. The μ' value of the Fe–Nb–B alloys becomes higher as Nb concentration increases. The soft magnetic properties, μ' above 35000 at 1 kHz and H_c below 5.0 Am^{-1} as well as high B_s above 1.55 T are obtained in the x and y ranges of 6.5–6.7 and 9.3–10 at%, respectively, for the nanocrystalline $Fe_{100-x-y}Nb_xB_y$ alloys. The best soft magnetic properties are obtained for the alloy with composition of $Fe_{84}Nb_{6.5}B_{9.5}$, so we choose $Fe_{84}Nb_{6.5}B_{9.5}$ as a basic composition in this study.

Next, the effect of the addition of P to the melt-spun $Fe_{84}Nb_{6.5}B_{9.5}$ alloy produced in the atmosphere is investigated. Amorphous Fe–Nb–B–P ribbons can be obtained for the alloys with P content of 0–2 at% by a melt-spinning method in the atmosphere.

Figure 2 shows an annealing temperature (T_a) dependence of (a) μ' at 1 kHz and (b) H_c for the $Fe_{84}Nb_{6.5}B_{9.5}$, $Fe_{84}Nb_{6.5}B_9P_{0.5}$ and $Fe_{84}Nb_{6.5}B_{8.5}P_1$ melt-spun alloys. As T_a increases, μ' increases and H_c decreases, shows the maximum and minimum values at T_a of 950 K, respectively, for the $Fe_{84}Nb_{6.5}B_{9.5}$ alloy. The optimum annealing tempera-

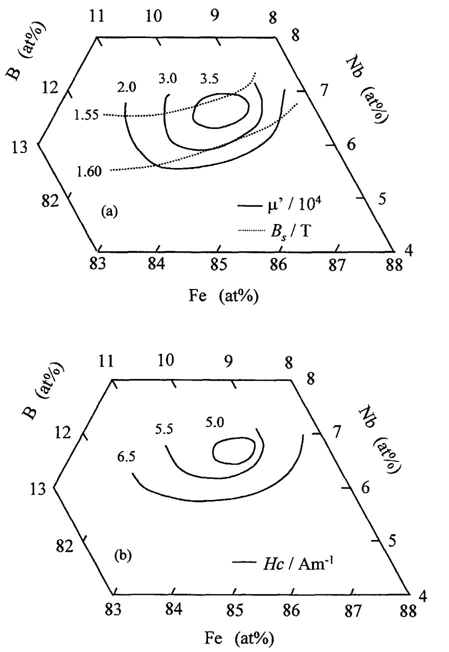

Fig. 1 The ternary diagrams of (a) permeability (μ') at a frequency of 1 kHz and saturation induction (B_s), and (b) coercive force (H_c) for the nanocrystalline Fe-Nb-B alloys produced by a melt-spinning method in the atmosphere and subsequent annealing.

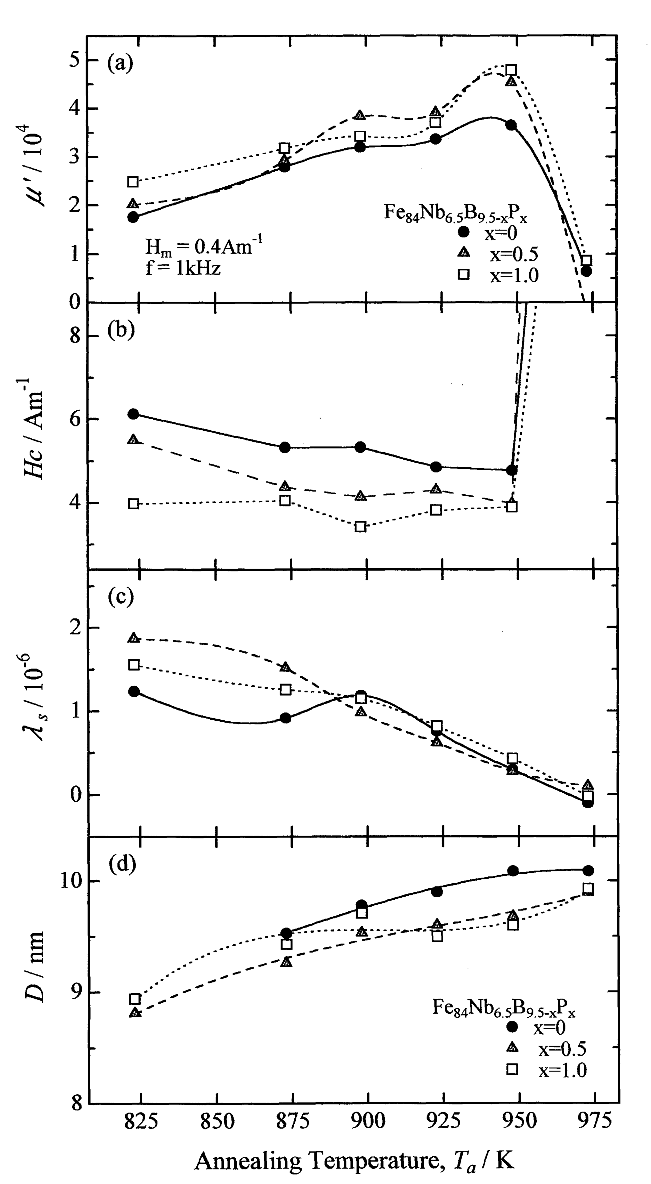

Fig. 2 The annealing temperature (T_a) dependence of (a) permeability (μ') at 1 kHz, (b) coercive force (H_c), (c) magnetostriction (λ_s) and (d) the mean grain size of the bcc phase (D), respectively, for the $Fe_{84}Nb_{6.5}B_{9.5}$, $Fe_{84}Nb_{6.5}B_9P_{0.5}$ and $Fe_{84}Nb_{6.5}B_{8.5}P_1$ alloys produced by melt-spinning in the atmosphere.

ture is almost unchanged by addition of P, and the good soft magnetic properties, μ' above 39000 and H_c below 5 Am^{-1} are obtained for the $Fe_{84}Nb_{6.5}B_{9.5-x}P_x$ (x = 0–1.0 at%) alloys after annealing at T_a of 950 K. It is noticed that the $Fe_{84}Nb_{6.5}B_{9.5-x}P_x$ (x = 0.5 and 1.0 at%) alloys show superior soft magnetic properties to the $Fe_{84}Nb_{6.5}B_{9.5}$ alloy in the wide T_a range of 825–950 K, and the $Fe_{84}Nb_{6.5}B_{8.5}P_1$ alloy exhibits the highest μ' of 46000 and lowest H_c of 3.6 Am^{-1} among these three alloys.

The T_a dependence of λ_s and mean grain size of the bcc phase (D) is shown in Figs. 2(c) and (d), respectively, for the $Fe_{84}Nb_{6.5}B_{9.5}$, $Fe_{84}Nb_{6.5}B_9P_{0.5}$ and $Fe_{84}Nb_{6.5}B_{8.5}P_1$ melt-spun alloys. The D value was calculated by using Scherrer's equation from the half-width of (110) X-ray reflection peak. The λ_s values decrease with increasing T_a and become almost zero at T_a of 975 K. These alloys show small and slightly positive magnetostriction about 0.5×10^{-6} upon annealing at the optimum temperature of 950 K. The D values become larger with increasing T_a, still keep small values about 10 nm even after annealing at T_a of 970 K. These results indicate that the melt-spun Fe–Nb–B–P alloys annealed at T_a of 950 K are the nanocrystalline soft magnetic alloys with small magnetostriction.

Figure 3 shows the changes in (a) B_s, (b) μ', (c) H_c, (d) λ_s, and (e) D as a function of P concentration (x) for the nanocrystalline $Fe_{84}Nb_{6.5}B_{9.5-x}P_x$, $Fe_{84}Nb_{6.7}B_{9.3-x}P_x$, $Fe_{84.5}Nb_6B_{9.5-x}P_x$ and $Fe_{84}Nb_6B_{10-x}P_x$ (x = 0–2 at%) alloys annealed at the optimum temperature. The B_s of the $Fe_{84}Nb_{6.5}B_{9.5}$, $Fe_{84}Nb_{6.7}B_{9.3}$, $Fe_{84.5}Nb_6B_{9.5}$ and $Fe_{84}Nb_6B_{10}$ alloys lies in the range of 1.58–1.63 T which is higher than that of the commercial amorphous $Fe_{78}Si_9B_{13}$ alloy, and almost unchanged by substitution of P for B. As P concentration (x) increase, μ' increases and H_c decreases, but a large amount of P substitution brings the decrease in μ' and the increase in H_c. The highest μ' and lowest H_c are obtained at the P concentration (x) of 0.7–1.5 at% for the $Fe_{84}Nb_{6.5}B_{9.5-x}P_x$ alloys, 0.5 at% for the $Fe_{84}Nb_{6.7}B_{9.3-x}P_x$ and $Fe_{84}Nb_6B_{10-x}P_x$ alloys, 1.0 at% for the $Fe_{84.5}Nb_6B_{9.5-x}P_x$ alloys, respectively. These results indicate that the soft magnetic properties of the nanocrystalline $Fe_{100-x}Nb_xB_y$ (x = 6–6.7, y = 9.3–10 at%) alloys are improved by 0.5–1.5 at% substitution of P for B.

As P concentration (x) increases, λ_s increases and D decreases slightly, still λ_s keeps the small values less than 1.0×10^{-6} at x = 1.5 at% for the $Fe_{84}Nb_{6.5}B_{9.5-x}P_x$ and $Fe_{84}Nb_6B_{10-x}P_x$ alloys. It is supposed that the increase in λ_s is one reason for the deterioration in soft magnetic properties by a large amount of substitution of P for B. The reduction of the D value is only 0.5 nm by 1 at% substitution of P for B, so we examined the change in microstructure by TEM observation. The fine crystallites with grain sizes of 6–18 nm are observed for both the $Fe_{84}Nb_{6.5}B_{9.5}$ and $Fe_{84}Nb_{6.5}B_{8.5}P_1$ alloys annealed at T_a of 950 K. The distribution of the grain size evaluated from bright field TEM images are shown in Fig. 4(a) and (b) for the $Fe_{84}Nb_{6.5}B_{9.5}$ and $Fe_{84}Nb_{6.5}B_{8.5}P_1$ alloys, respectively. The mean grain sizes are estimated at 10.1 and 9.3 nm for the $Fe_{84}Nb_{6.5}B_{9.5}$ and $Fe_{84}Nb_{6.5}B_{8.5}P_1$ alloys, respectively. These values are almost the same as those calculated from the half width of X-ray diffraction peaks shown in Fig. 3(e), and it can be concluded that the mean grain size

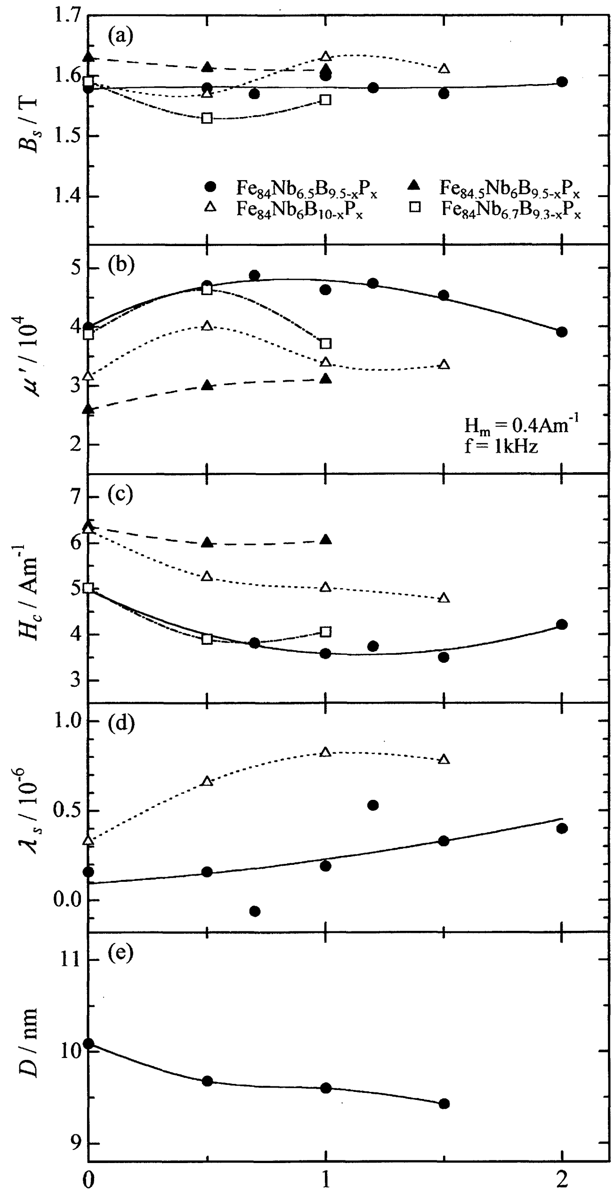

Fig. 3 The changes in (a) B_s, (b) μ', (c) H_c, (d) λ_s, and (e) D as a function of P concentration (x) for the nanocrystalline $Fe_{84}Nb_{6.5}B_{9.5-x}P_x$, $Fe_{84}Nb_{6.7}B_{9.3-x}P_x$, $Fe_{84.5}Nb_6B_{9.5-x}P_x$ and $Fe_{84}Nb_6B_{10-x}P_x$ (x = 0–2 at%) alloys annealed at the optimum temperature of 950 K.

of the $Fe_{84}Nb_{6.5}B_{9.5}$ alloy annealed at 950 K is reduced by substitution of P for B.

Figures 5(a) and (b) show the changes in the crystallization temperature (T_x) and Curie temperature (T_c) as a function of P concentration (x) for the amorphous $Fe_{84}Nb_{6.5}B_{9.5-x}P_x$ melt-spun alloys in the as-quenched state and after annealing at 673 and 723 K. T_c values were evaluated from the μ' versus temperature curve. T_x decreases by substitution of P for B. It has been reported[9] that D is strongly related to T_x, and decreases with decreasing T_x for the nanocrystalline Fe–TM–Zr–B (TM=Ti, V, Cr, Mn) alloys. It is noticed that the similar tendency is observed for the $Fe_{84}Nb_{6.5}B_{9.5-x}P_x$ alloys. On the other hand, T_c of the amorphous $Fe_{84}Nb_{6.5}B_{9.5}$ alloy increases by substitution of P for B in the as-quenched and annealed states. These results suggest that T_c of the resid-

Table 1 Saturation induction (B_s), relative permeability (μ'), coercive force (H_c), magnetostriction (λ_s) and core loss (W) of the nanocrystalline Fe–Nb–B and Fe–Nb–B–P alloys produced by melt-spinning in the atmosphere and subsequent annealing.

Composition	B_s/T	μ'^{a}	H_c/Am^{-1}	$\lambda_s \times 10^6$	$W_{1.33/50}{}^{b}$/Wkg^{-1}
$Fe_{84}Nb_{6.5}B_{9.5}$	1.58	39900	5.0	0.2	0.10
$Fe_{84}Nb_{6.7}B_{9.3}$	1.59	38800	4.8	0.1	0.12
$Fe_{84}Nb_{6.5}B_9P_{0.5}$	1.60	47100	3.9	0.2	0.09
$Fe_{84}Nb_{6.5}B_{8.5}P_1$	1.60	46300	3.6	0.2	0.09

a: 1 kHz, 0.4 Am^{-1}
b: 50 Hz, 1.33 T

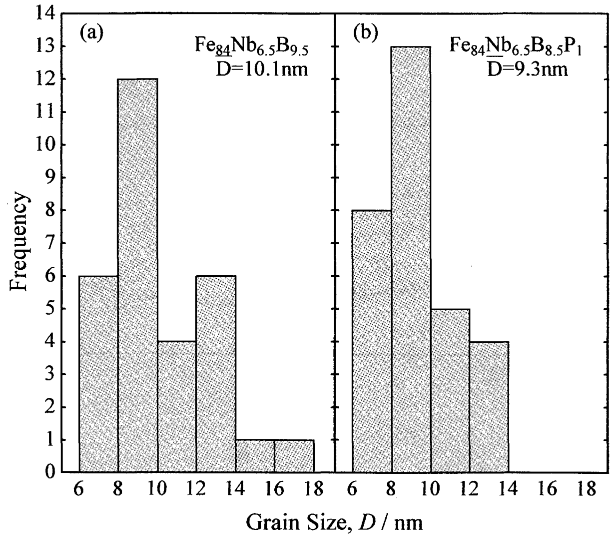

Fig. 4 The distribution of the grain size evaluated by counting the grains in the TEM images for the (a) $Fe_{84}Nb_{6.5}B_{9.5}$ and (b) $Fe_{84}Nb_{6.5}B_{8.5}P_1$ alloys after annealing at 950 K.

ual amorphous phase increases as well even after annealing at the optimum temperature.

Next, the core losses (W) of the Fe–Nb–B–P alloys at a frequency of 50 Hz was investigated because the application as a core material for the pole transformer demands the soft magnetic properties at low frequencies of 50–60 kHz. Figure 6 shows the changes in W as a function of maximum induction (B_m) for the nanocrystalline $Fe_{84}Nb_{6.5}B_{9.5}$ and $Fe_{84}Nb_{6.5}B_{8.5}P_1$ alloys, along with that of the amorphous $Fe_{78}Si_9B_{13}$ alloy for comparison. The nanocrystalline $Fe_{84}Nb_{6.5}B_{8.5}P_1$ alloy shows lower W than the $Fe_{84}Nb_{6.5}B_{9.5}$ alloy in the B_m range of 1.1–1.4 T, and exhibits a W of 0.09 Wkg^{-1} at B_m of 1.3 T, which is extremely lower than that of the amorphous $Fe_{78}Si_9B_{13}$ alloy.

Finally, the magnetic properties of the representative nanocrystalline Fe–Nb–B and Fe–Nb–B–P alloys produced by melt-spinning in the atmosphere and subsequent annealing, are summarized in Table 1. The $Fe_{84}Nb_{6.5}B_9P_{0.5}$ and $Fe_{84}Nb_{6.5}B_{8.5}P_1$ alloys show good soft magnetic properties, μ' of 46000–47000 at 1 kHz, H_c of 3.6–3.9 Am^{-1} and the core loss ($W_{1.33/50}$) of 0.09 Wkg^{-1} at 1.33 T and 50 Hz as well as high B_s of 1.60 T. Therefore, these nanocrystalline Fe–Nb–B–P alloys are suitable for a core material for the pole transformers.

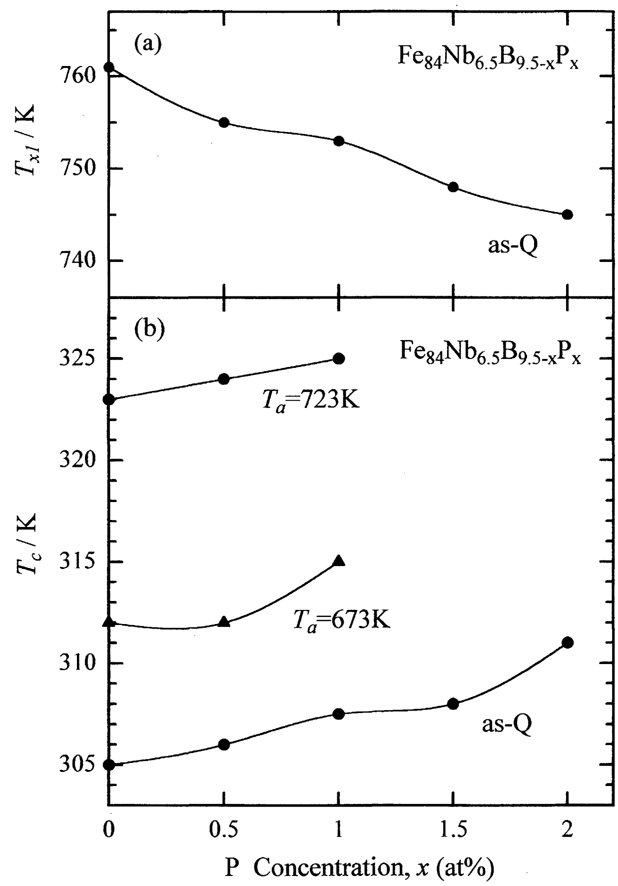

Fig. 5 The changes in (a) the crystallization temperature (T_x) and (b) Curie temperature (T_c) as a function of P concentration (x) for the amorphous $Fe_{84}Nb_{6.5}B_{9.5-x}P_x$ melt-spun alloys in the as-quenched state and after annealing at 673 and 723 K.

4. Conclusions

The soft magnetic properties of the nanocrystalline Fe–Nb–B and Fe–Nb–B–P alloys produced by melt-spinning in the atmosphere and subsequent annealing have been investigated. The results obtained are summarized as follows.

(1) The nanocrystalline $Fe_{100-x-y}Nb_xB_y$ (x = 5–7, and y = 9–11 at%) ternary alloys annealed at an optimum temperature show good soft magnetic properties, relative permeability (μ') above 35000 at a frequency of 1 kHz and coercive force (H_c) below 5.0 Am^{-1}, as well as high saturation magnetic induction (B_s) above 1.55 T, in the x and y ranges of 6.0–6.7 and 9.0–10 at%, respectively.

(2) The soft magnetic properties of the nanocrystalline $Fe_{100-x}Nb_xB_y$ (x = 6.0–6.7, y = 9.3–10 at%) alloys are

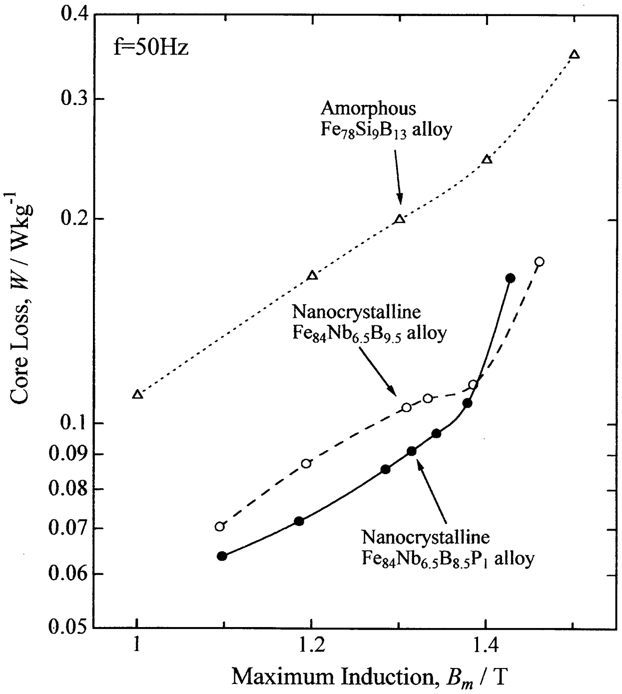

Fig. 6 The changes in the core loss (W) at a frequency of 50 Hz as a function of maximum induction (B_m) for the nanocrystalline $Fe_{84}Nb_{6.5}B_{9.5}$ and $Fe_{84}Nb_{6.5}B_{8.5}P_1$ alloys annealed at 950 K, along with that of the amorphous $Fe_{78}Si_9B_{13}$ alloy.

improved by 0.5–1.5 at% substitution of B for P, without decreasing their B_s. The magnetostriction increases and the mean grain size of bcc-Fe phase decreases slightly with increasing P concentration for the $Fe_{84}Nb_{6.5}B_{9.5-x}P_x$ and $Fe_{84}Nb_6B_{10-x}P_x$ alloys.

(3) The $Fe_{84}Nb_{6.5}B_9P_{0.5}$ and $Fe_{84}Nb_{6.5}B_{8.5}P_1$ alloys show good soft magnetic properties, μ' of 46000–47000 at 1 kHz, H_c of 3.6–3.9 Am^{-1} and the core loss ($W_{1.33/50}$) of 0.09 Wkg^{-1} at 1.33 T and 50 Hz as well as high B_s of 1.60 T. The $W_{1.33/50}$ values of these nanocrystalline alloys are extremely lower than that of the amorphous $Fe_{78}Si_9B_{13}$ alloy, suggesting that these nanocrystalline Fe–Nb–B–P alloys are suitable for a core material for pole transformers.

Acknowledgements

This work was supported by a Grant-in-Aid from the New Energy and Industrial Technology Development Organization (NEDO).

REFERENCES

1) Y. Yoshizawa, S. Oguma and K. Yamauchi: J. Appl. Phys. **64** (1988) 6044–6046.
2) K. Suzuki, A. Makino, A. Inoue and T. Masumoto: J. Appl. Phys. **74** (1993) 3316–3322.
3) A. Makino, K. Suzuki, A. Inoue, Y. Hirotu and T. Masumoto: J. Magn. Magn. Mater. **133** (1994) 329–332.
4) A. Makino, T. Bito, A. Kojima, A. Inoue and T. Masumoto: J. Magn. Magn. Mater. **215–216** (2000) 288–292.
5) A. Makino, T. Bito, A. Kojima, A. Inoue and T. Masumoto: J. Appl. Phys. **87** (2000) 7100–7102.
6) A. Makino, A. Inoue and T. Masumoto: Nano Structured Materials **6** (1994) 985–988.
7) A. Makino, T. Bito, A. Inoue and T. Masumoto: J. Appl. Phys. **81** (1997) 2736–2739.
8) K. Suzuki, A. Makino, A. Inoue and T. Masumoto: J. Phys. Soc. Jpn. **18** (1944) 800–804.
9) T. Bito, N. Nakazawa, A. Makino, A Inoue and T. Masumoto: J. Appl. Phys. **85** (1997) 5127–5129.